SUPPORTING INFORMATION

Structural, spectral and magnetic properties of Ni(II), Co(II) and Cd(II) compounds with imidazole derivatives and silanethiolate ligands

D. Kowalkowska,[a] A. Dołęga, [a] N. Nedelko,[b] Z. Hnatejko,[c] Ł. Ponikiewski,[a] A. Matracka,[a] A. Ślawska-Waniewska,[b] A. Strągowska,[a] K. Słowy[a], M. Gazda[d] and A. Pladzyk *[a]

[a] *Department of Inorganic Chemistry, Chemical Faculty, Gdańsk University of Technology, Narutowicza Str. 11/12, 80-233 Gdańsk, Poland*
[b] *Institute of Physics, Polish Academy of Sciences, Aleja Lotnikow 32/46, 02-668 Warsaw, Poland*
[c] *Faculty of Chemistry, Adam Mickiewicz University, Umultowska 89b, 61-414 Poznań, Poland*
[d] *Department of Solid State Physics, Faculty of Applied Physics and Mathematics, Gdańsk University of Technology, Narutowicza Str. 11/12, 80-233 Gdańsk, Poland*

To whom correspondence should be addressed. Email: agnieszka.pladzyk@pg.gda.pl

Supplementary Index

1. PHYSICAL MEASUREMENT

^{1}H NMR (internal TMS) spectra were recorded with a Varian Unity 500 MHz spectrometers at room temperature. The SpinWorks 3.17 [1] software and Simulation Module Nummrit [2] were used for the simulation of the NMR spectra.

2. EXPERIMENTAL PART

Synthesis of 1,4-bis(imidazol-1-yl)-butane

A mixture of imidazole (3.40 g, 50 mmol) and sodium hydroxide (2.00 g, 50 mmol) in dimethyl sulfoxide (10 mL) was stirred at 75 °C for 1.5 h under an atmosphere of N_2. Then, 1,4-dibromobutane (5.40 g, 25 mmol) was added drop-wise to avoid the rise of the temperature (the reaction is very exothermic) and the mixture was stirred until it solidified. The mushy solid was extracted into toluene (3×100 mL) with excessive stirring. The combined organic extracts were left for crystallization at -25 °C. After some days a colorless crystals of 1,4-bis(imidazol-1-yl)-butane monohydrated (bbi) were collected. M.p. 81-83 °C.

3. SUPPORTING FIGURES

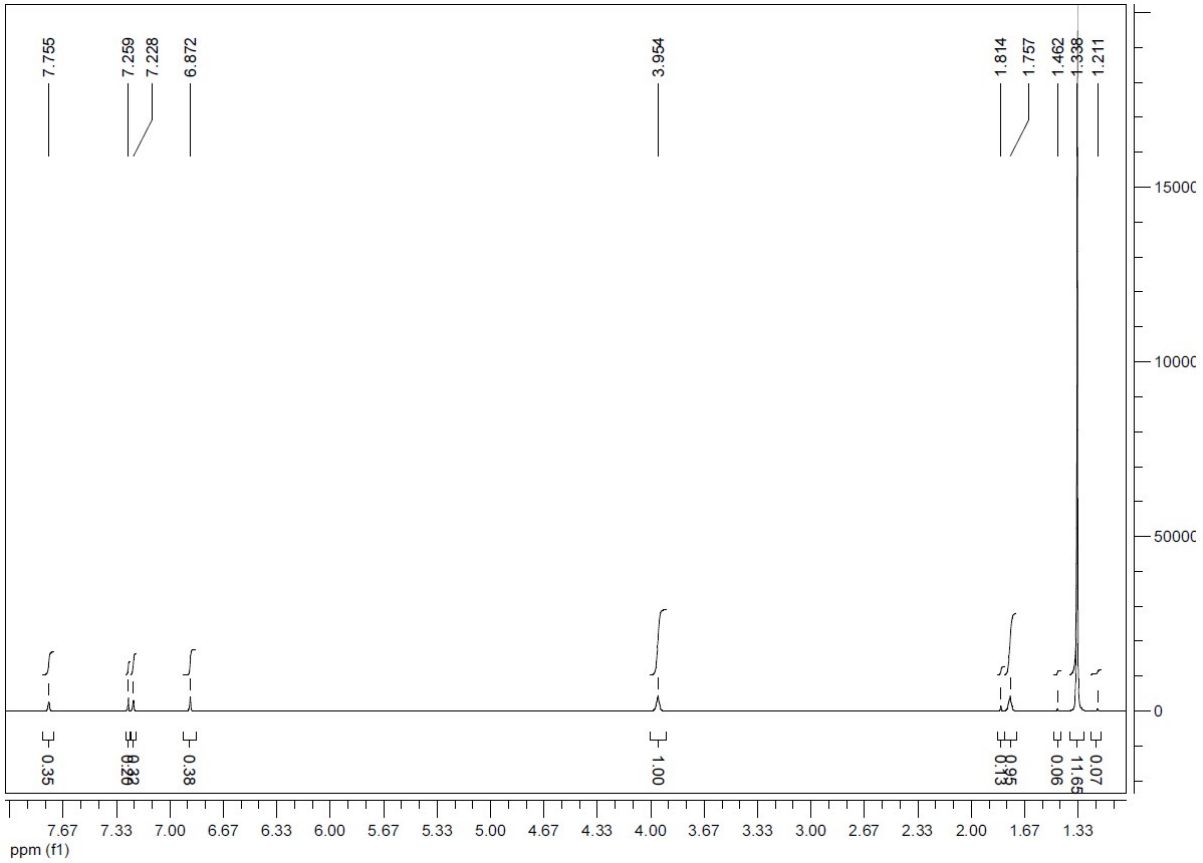

Fig. S1. ^{1}H NMR spectrum of 1,4-bis(imidazol-1-yl)-butane (bbi).

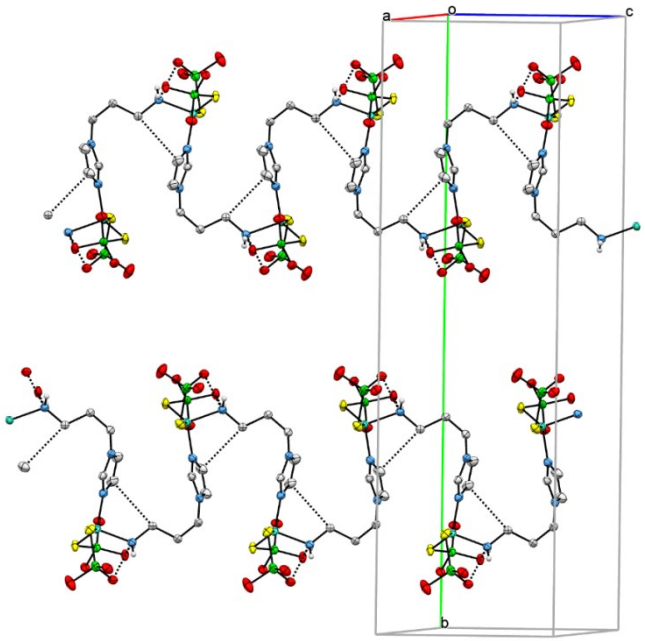

Fig. S2. The crystal packing of **1** along *b* axis. H atoms and *t*Bu groups omitted for clarity (S-yellow, O-red, N-blue, Si-green, Ni-celadon, C - grey).

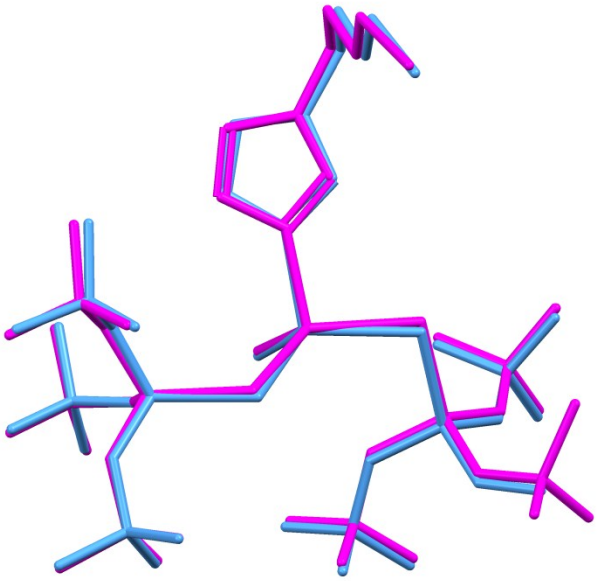

Fig. S3. The overlays of unit cells **1** (pink) and **2** (blue) structures. H atoms omitted for clarity.

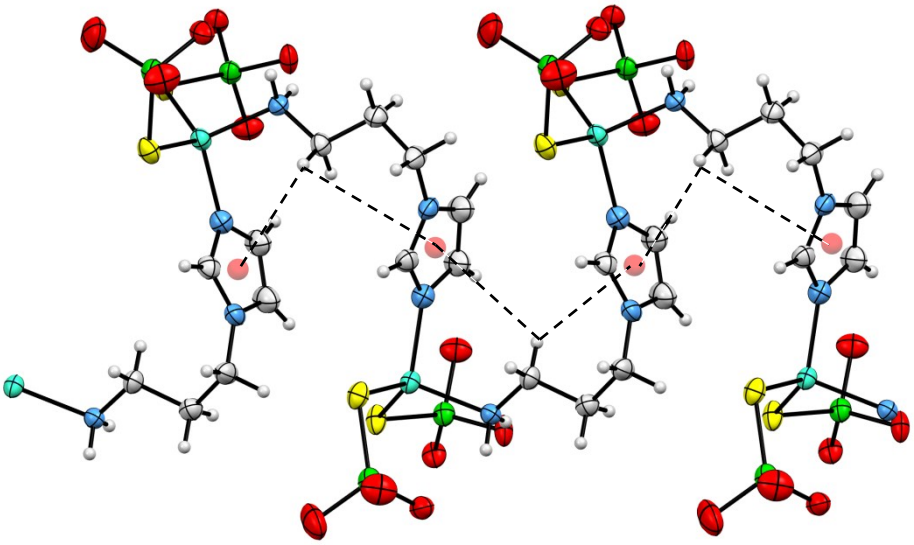

Fig. S4. The view on the polymeric chain of compound **2** with additional C–H···π interactions showed as dashed lines. *t*BuO groups omitted for clarity.

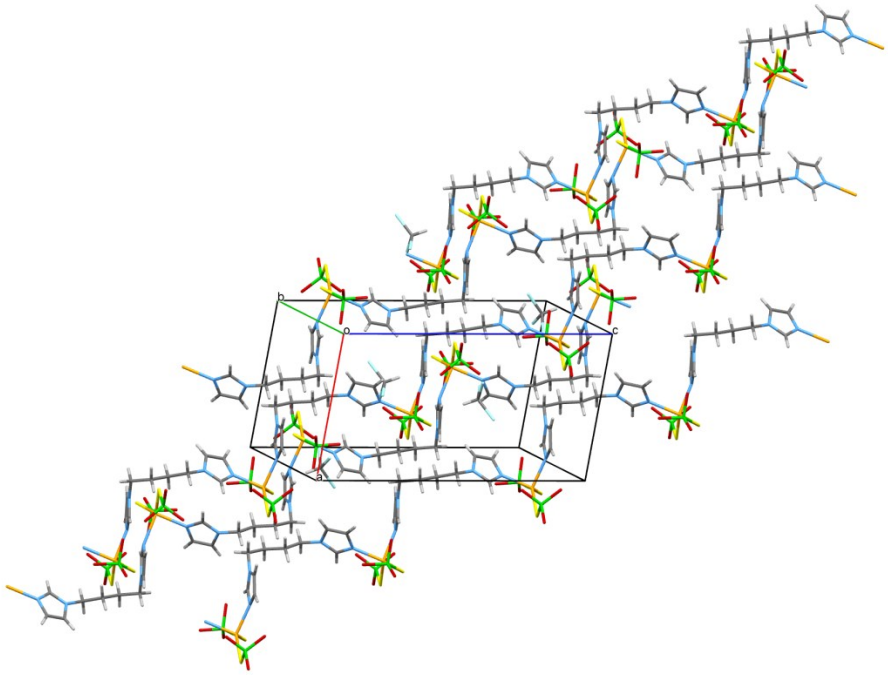

Fig. S5. The crystal packing of **4** along *b* axis. *t*BuO groups omitted for clarity.

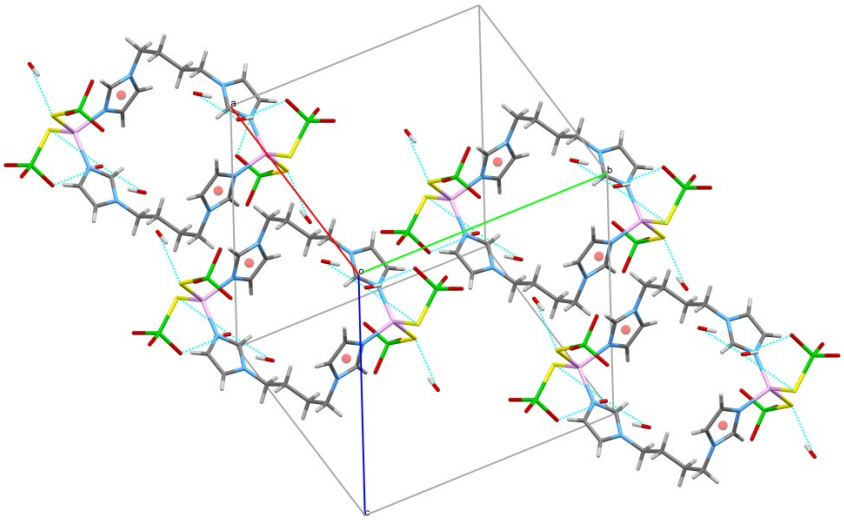

Fig. S6. The crystal packing of **5** along *a* axis with the net of hydrogen bonding and C–H···π interactions. H atoms in methanol and *t*BuO groups omitted for clarity.

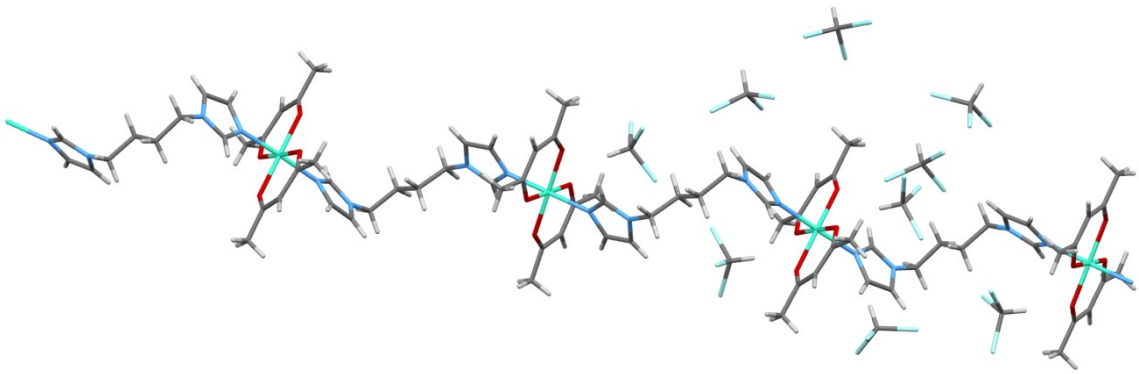

Fig. S7. The view on the polymeric chain of **6**.

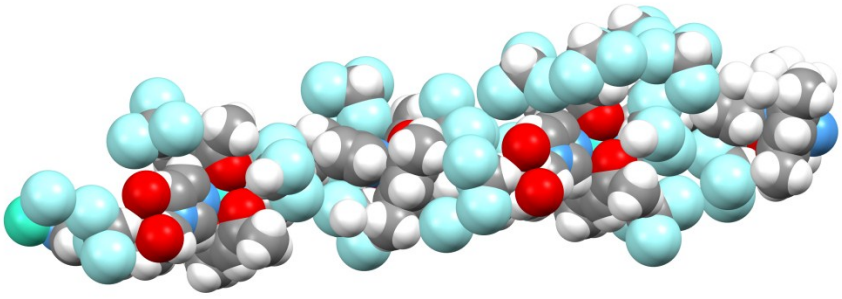

Fig. S8. The spacefill view on the polymeric chain of **6**. H atoms of $CHCl_3$ molecules omitted for clarity (O-red, N-blue, Ni-celadon, Cl – bluish, C- grey, H - white).

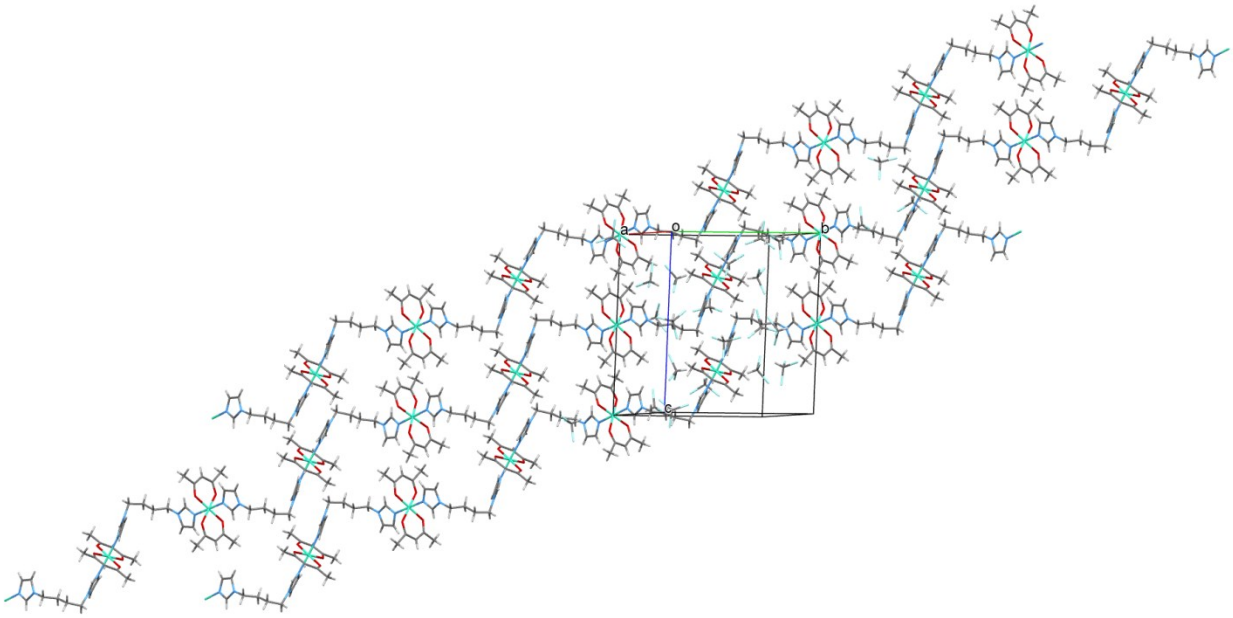

Fig. S9. The crystal packing of **6** along *a* axis.

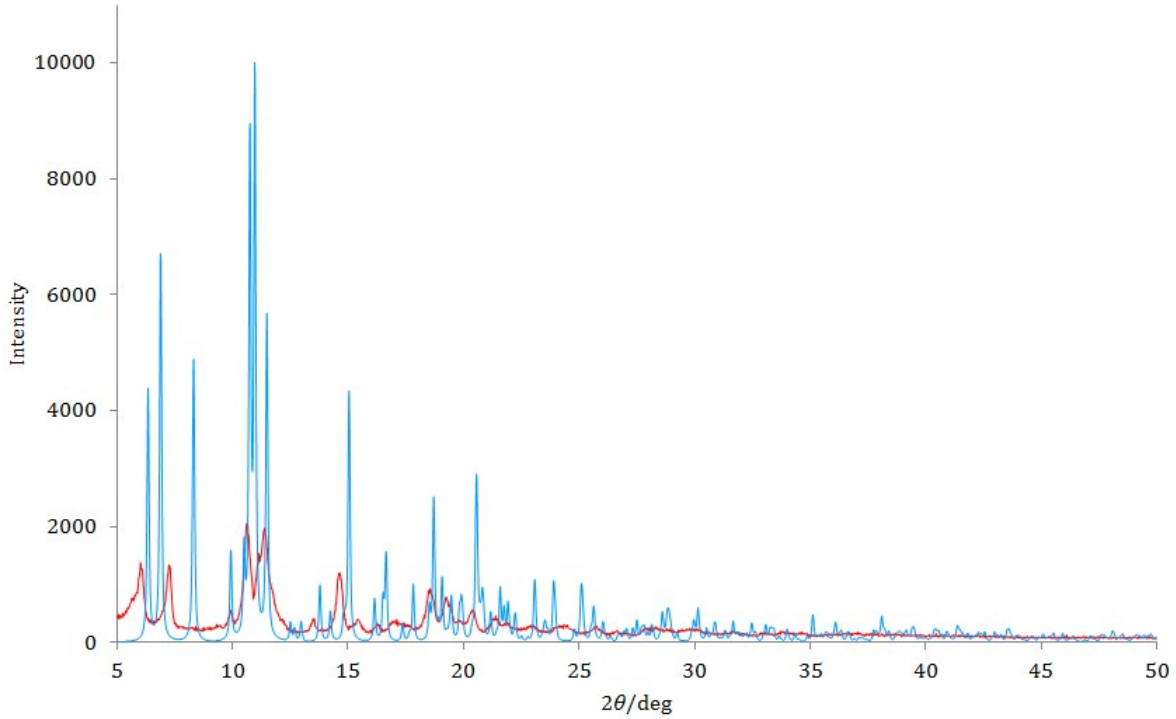

Fig. S10. The powder X-ray pattern of complex **1**: measured – red line; the simulated pattern of complex **1** derived from single crystal data – blue line.

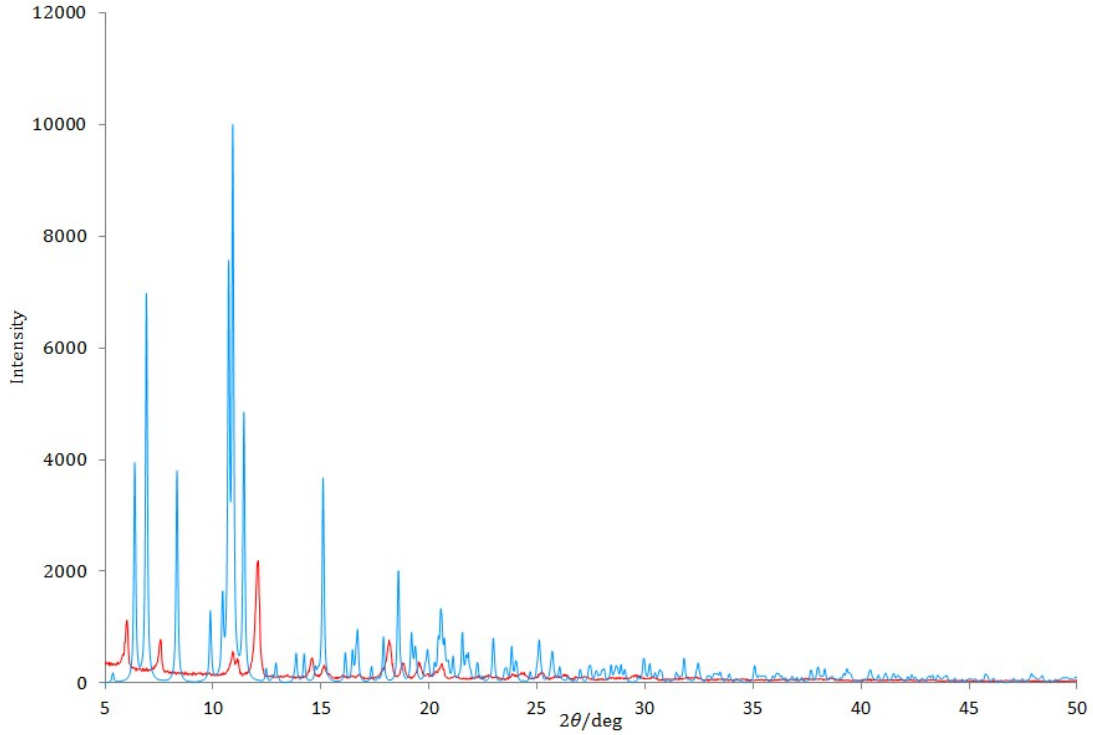

Fig. S11. The powder X-ray pattern of complex **2**: measured – red line; the simulated pattern of complex **2** derived from single crystal data – blue line.

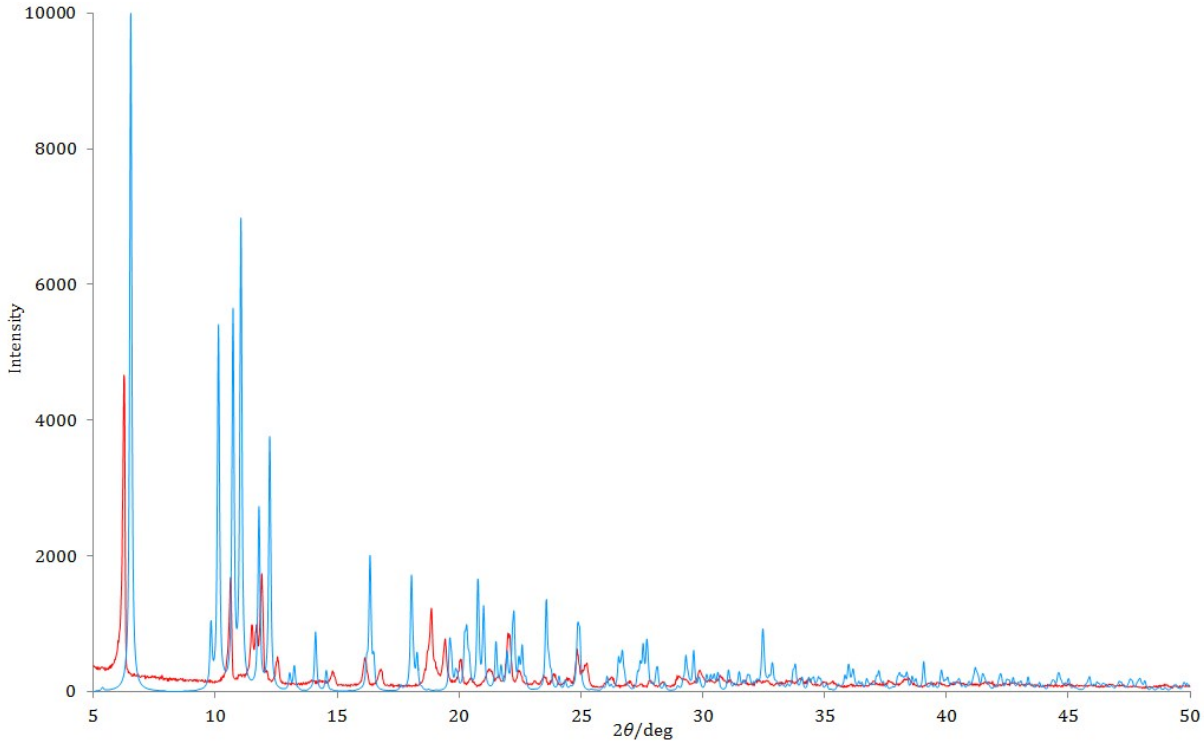

Fig. S12. The powder X-ray pattern of complex **3**: measured – red line; the simulated pattern of complex **3** derived from single crystal data – blue line.

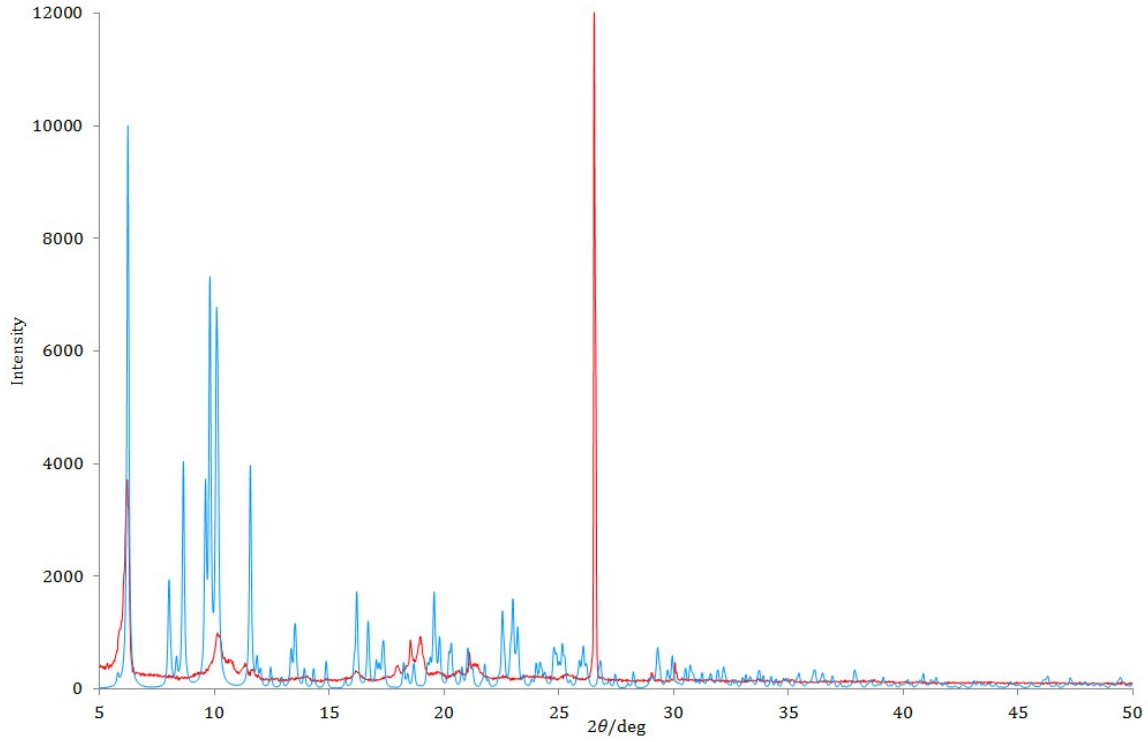

Fig. S13. The powder X-ray pattern of complex **4**: measured – red line; the simulated pattern of complex **4** derived from single crystal data – blue line.

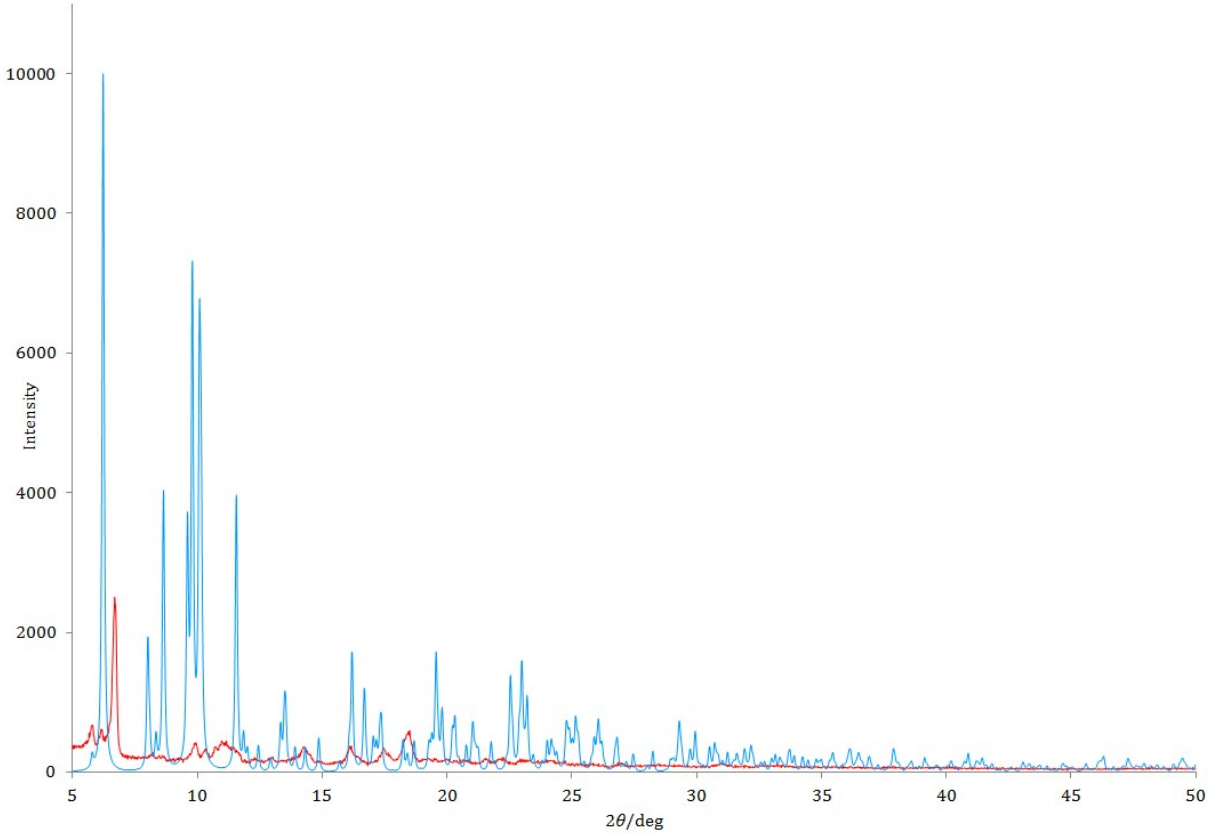

Fig. S14. The powder X-ray pattern of complex **5**: measured – red line; the simulated pattern of complex **5** derived from single crystal data – blue line.

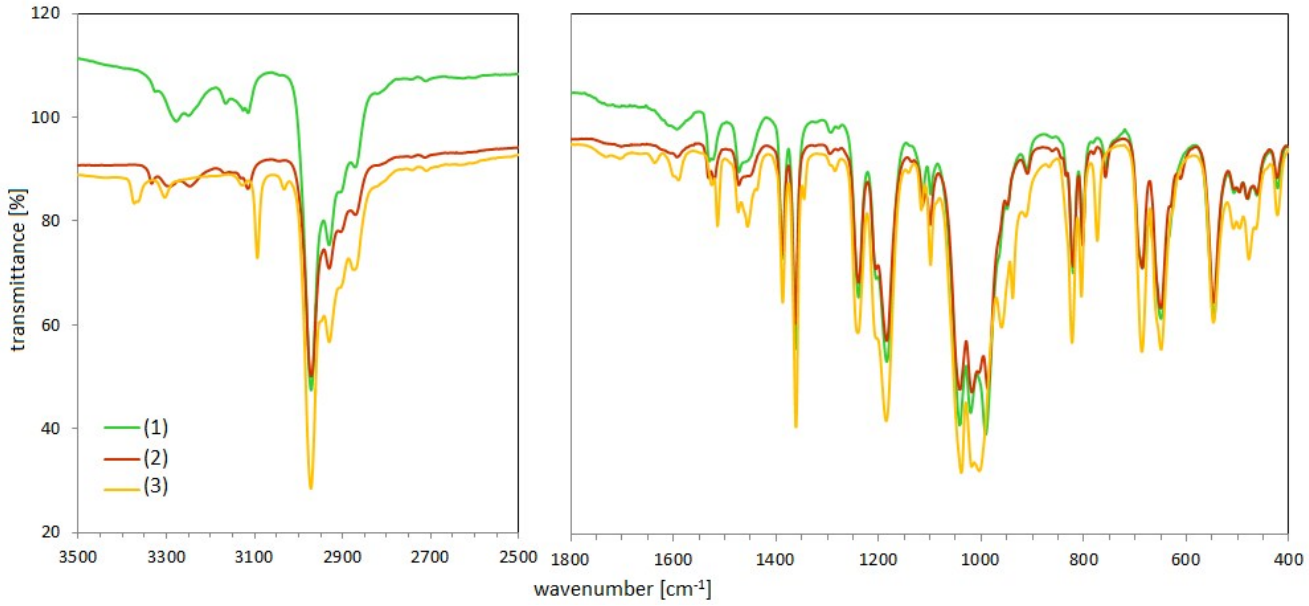

Fig. S15. FTIR spectrum of complex **1-3** in the range of 4000-400 cm^{-1}.

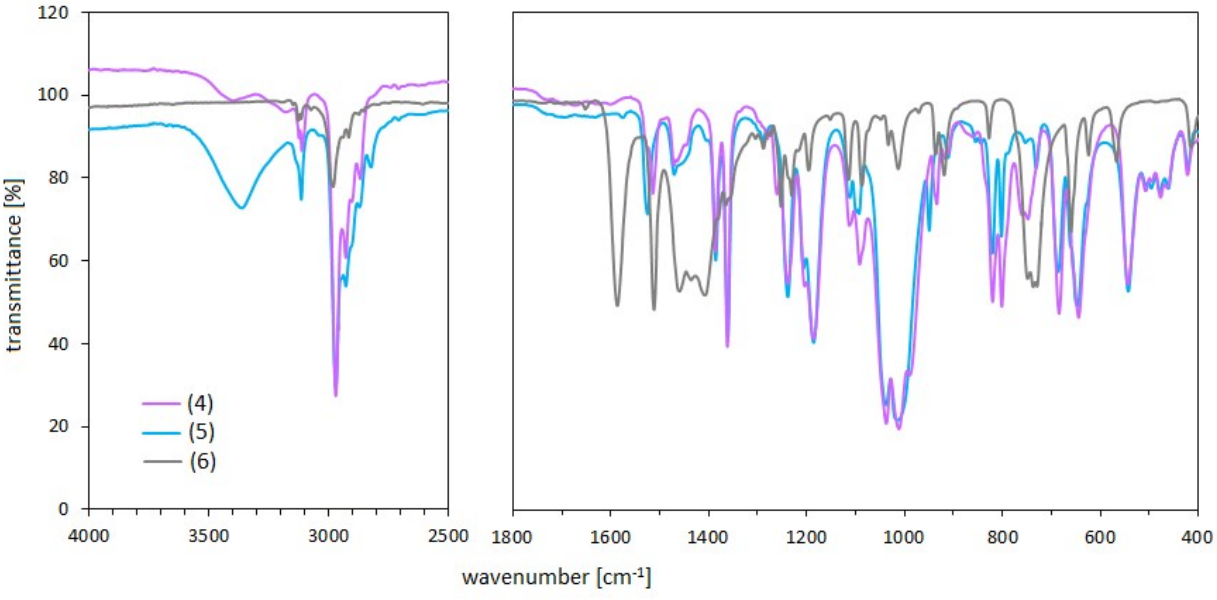

Fig. S16. FTIR spectrum of complex **4-6** in the range of 4000-400 cm^{-1}.

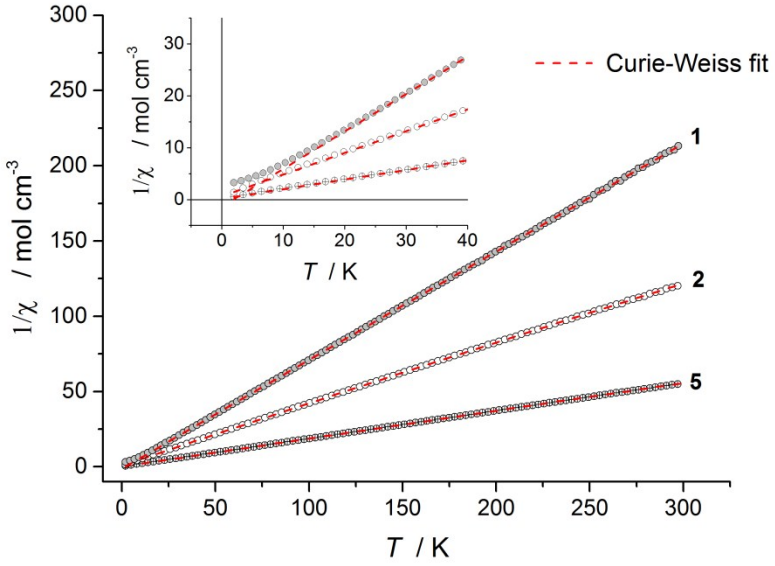

Fig. S17. Reciprocal molar susceptibility ($1/\chi$) versus temperature for **1**, **2** and **5**. Dashed lines are the best Curie-Weiss fit to the data (see text); the inset shows a magnification of the low temperature range.

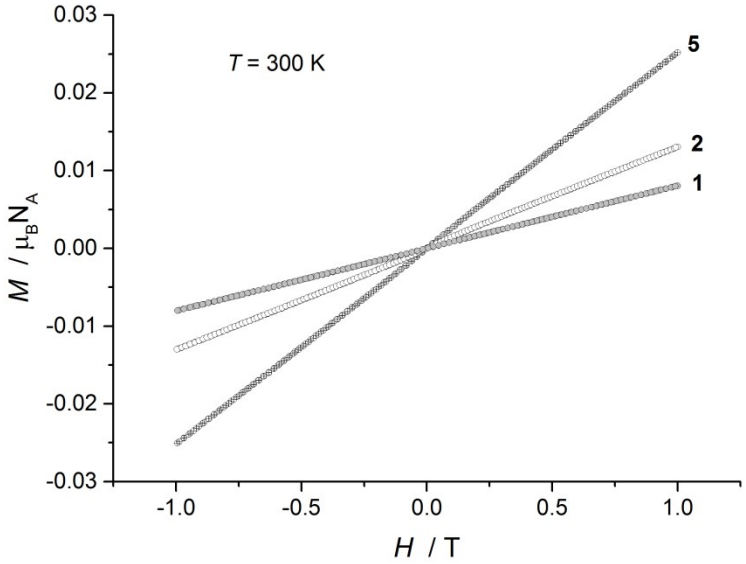

Fig. S18. Magnetization curves for samples **1**, **2** and **5** measured at 300 K.

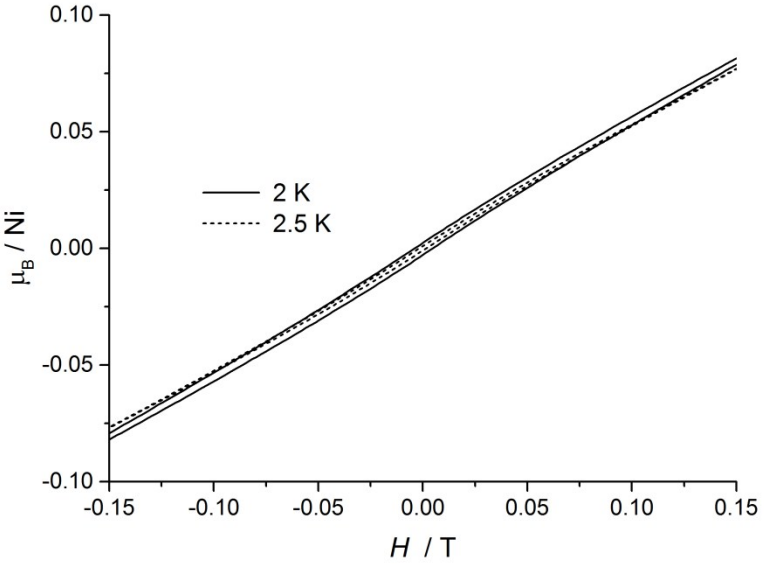

Fig. S19. Magnetization curves for **1** (a low field range) measured at 2 and 2.5 K.

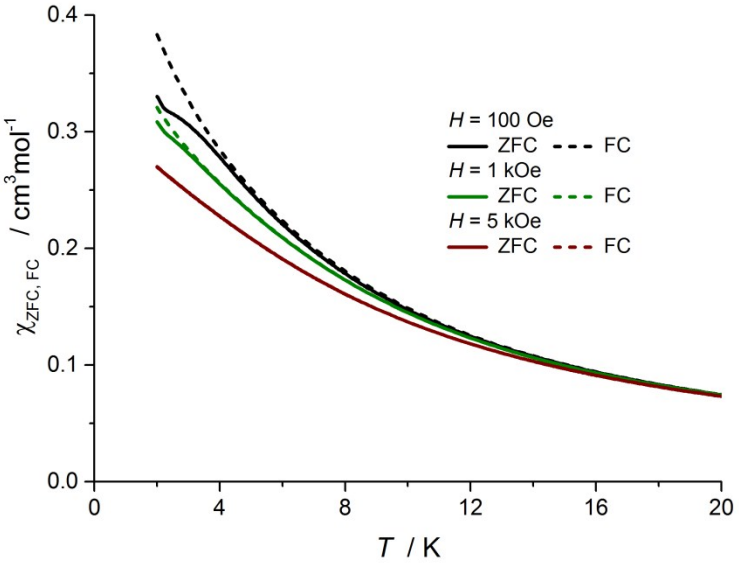

Fig. S20. Temperature dependences of χ_{ZFC} and χ_{FC} magnetic susceptibility measured in selected fields (100 Oe, 1 kOe and 5 kOe) for **1**.

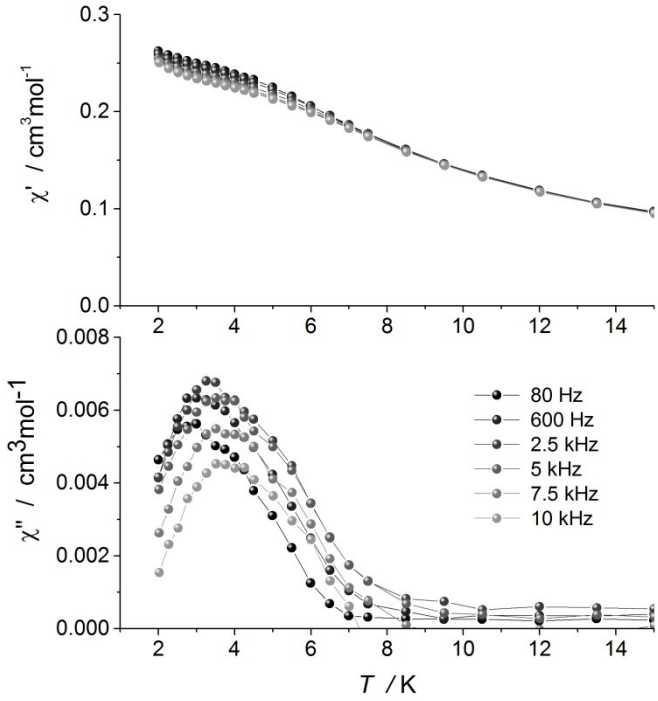

Fig. S21. Temperature dependences of real χ' and imaginary χ'' components of the susceptibility for sample **1** at selected frequencies (measured in zero external *dc* field for exciting field of 3 Oe).

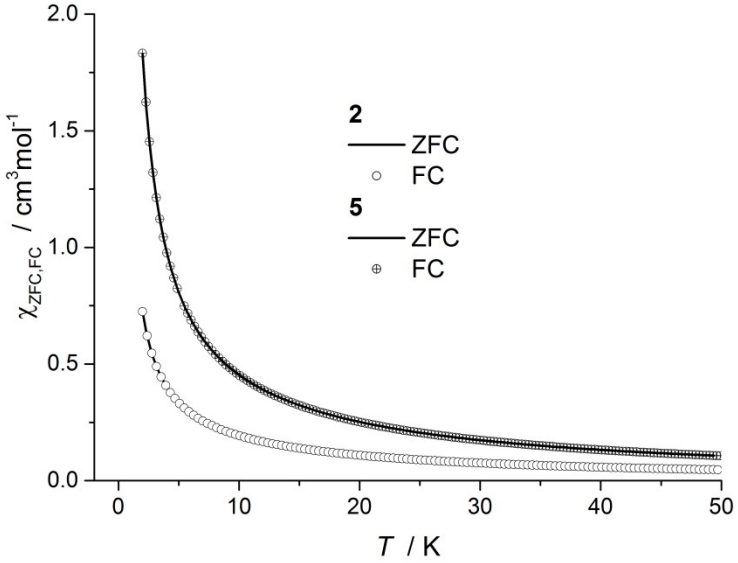

Fig. S22. Temperature dependences of χ_{ZFC} and χ_{FC} magnetic susceptibility measured in H = 1 kOe for **2** and **5**.

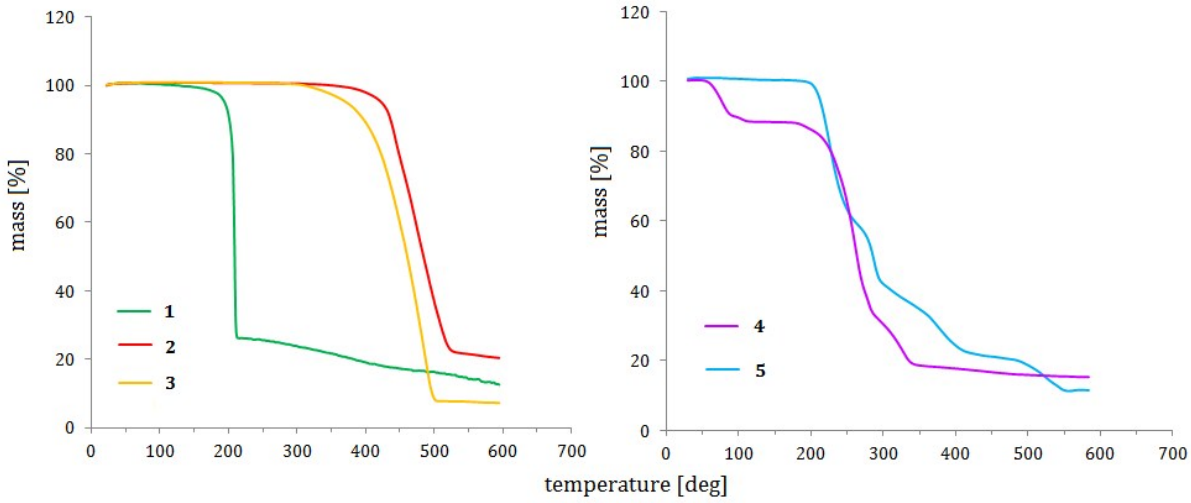

Fig. S23. Thermogravimetric curves of 1-5 obtained at a heating rate of 10 K min^{-1}.

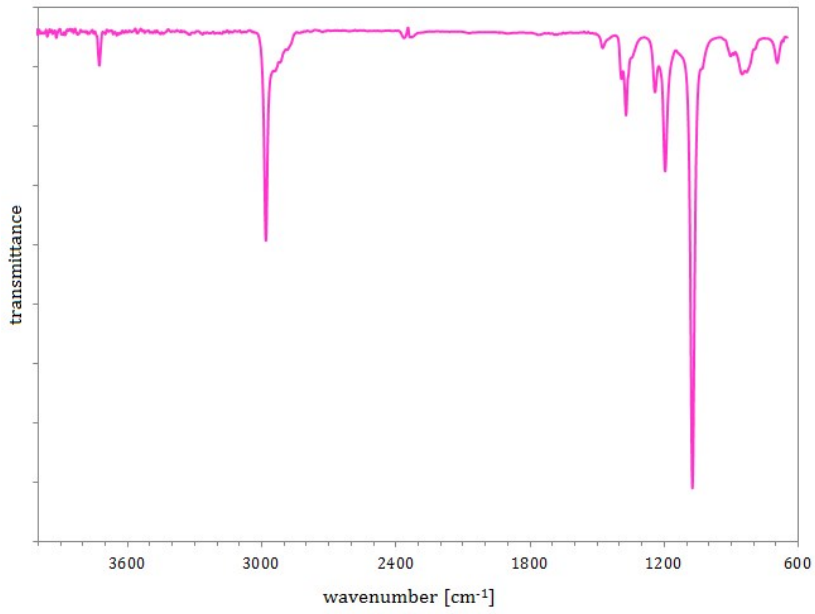

Fig. S24. FTIR spectrum of the volatiles evolving during TG analysis of **5** recorded at 240 °C.

4. EMPIRICAL EQUATIONS USED IN THE FITTING PROCEDURES OF VARIABLE TEMPERATURE MAGNETIC SUSCEPTIBILITIES DATA.

De Neef's expressions for S = 1 uniform Heisenberg chain with Zero Field Splitting based on the Hamiltonian[1]:

$$H = -2J\sum_i \hat{S}_i\hat{S}_{i+1} - \Delta\sum_i\left(\hat{S}_{iz}^2 - \frac{2}{3}\right) + \alpha H\sum_i \hat{S}_{iz}$$

where $\Delta = -D$ and $\alpha = g\mu_B$.

$$\chi(J,\Delta) = N_A\left[\chi(J,0) + \chi(0,\Delta) + \frac{1}{3}\alpha^2\beta\sum_{i,j}\frac{b_{ij}J^i\Delta^j\beta^{i+j}}{3^{i+j}(i+j)!} - \frac{2\beta\alpha^2}{3}\right] + \chi_{TIP} \qquad \text{(A1)}$$

$$\chi(0,\Delta) = \frac{2\beta\alpha^2}{2 + e^{-\Delta\beta}} \qquad \text{(A2)}$$

$$\chi(J,0) = \alpha^2\sum_i \frac{d_i J^{i-1}\beta^i}{3^i i!} \qquad \text{(A3)}$$

where $\beta = \frac{1}{k_B T}$.

Coefficients for the magnetic susceptibility in eq. A1,A3:

i	d_i	b_{i1}	b_{i2}	b_{i3}	b_{i4}	b_{i5}
1	2	64	0	-768	960	24192
2	32	1008	3744	-25440	-164592	
3	240	3840	174720	292608		
4	-3072	-181440	1841472			
5	-62400	225792				
6	2820096					

Empirical equation for the magnetic susceptibility of mononuclear S = 3/2 system that includes Zero Field Splitting based on the Hamiltonian[2]:

$$H = g\mu_B\hat{S}\cdot H + D\left[\hat{S}_z^2 - \frac{S(S+1)}{3}\right].$$

$$\chi_{calcd} = \frac{\chi_z + 2\chi_{xy}}{3} + \chi_{TIP} \qquad \text{(B1)}$$

$$\chi_z = \frac{N_A g_z^2\mu_B^2}{k_B T}\left[\frac{1 + 9e^{-2D/k_B T}}{4\left(1 + e^{-2D/k_B T}\right)}\right] \qquad \text{(B2)}$$

$$\chi_{xy} = \frac{N_A g_{xy}^2\mu_B^2}{k_B T}\left[\frac{4 + (3k_B T/D)\left(1 - e^{-2D/k_B T}\right)}{4\left(1 + e^{-2D/k_B T}\right)}\right] \qquad \text{(B3)}$$

An expression for the exchange-influenced magnetic susceptibility components[3]:

$$\chi_{z,xy}^{'} = \frac{\chi_{z,xy}}{1 - \left(\frac{2zJ^{'}}{N_A g_{z,xy}^{2} \mu_B^2}\right)\chi_{z,xy}} \qquad \text{(B4)}$$

where J' is the interaction parameter between nearest magnetic species and z is the number of nearest neighbors.

5. STRUCTURAL DATA

Table S1 Selected interatomic distances (Å) and angles (°) for **1**-**5**

	1 (M=Ni)	**2** (M=Co)	**3** (M=Cd)	**4** (M=Cd)	**5** (M=Co)
Bond length [Å]					
M(1)–N(1)	2.012(3)^{i}	2.020(4)	2.238(4)	2.259(4)	2.029(4)
M(1)–N(2)	1.988(3)	2.042(4)			
M(1)–N(3)					2.017(4)
M(2)–N(3)			2.342(4)^{iiiii}	2.257(4)	
M(2)–N(4)			2.247(4)		
M(1)–N(5)					
M(1)–N(6)			2.340(4)		
M(1)–S(1)	2.2651(10)	2.2884(14)	2.4560(14)	2.4728(13)	2.299(3)
M(1)–S(2)	2.2905(11)	2.3042(13)	2.4828(13)	2.4510(13)	2.300(3)
M(2)–S(3)			2.4906(13)		
M(2)–S(4)			2.4647(14)		
Si(1)–S(1)	2.0870(15)	2.0813(17)	2.0779(18)	2.0659(17)	2.089(3)
Si(2)–S(2)	2.0840(15)	2.084(2)	2.0824(19)	2.0907(17)	2.077(3)
Si(3)–S(3)			2.0795(19)		
Si(4)–S(4)			2.0826(18)		
Si(1)–O(1)	1.634(3)	1.637(4)	1.627(4)	1.614(4)	1.636(4)
Si(1)–O(2)	1.631(3)	1.616(3)	1.639(4)	1.627(4)	1.609(4)
Si(1)–O(3)	1.624(3)	1.625(4)	1.607(4)	1.622(5)	1.620(4)
Si(2)–O(4)	1.630(3)	1.627(3)	1.636(3)	1.629(3)	1.619(4)
Si(2)–O(5)	1.625(3)	1.605(4)	1.631(4)	1.625(3)	1.621(4)
Si(2)–O(6)	1.642(3)	1.640(5)	1.629(3)	1.628(3)	1.632(4)
Si(3)–O(7)			1.638(4)		
Si(3)–O(8)			1.621(4)		
Si(3)–O(9)			1.632(3)		
Si(4)–O(10)			1.623(4)		
Si(4)–O(11)			1.635(4)		
Si(4)–O(12)			1.638(4)		
Bond angles [deg]					
N(1)–M(1)–N(2)	99.82(13)^{i}	102.89(17)			
N(1)–M(1)–N(3)				89.95(16)	105.10(16)

N(1)–M(1)–N(6)			93.17(15)		
N(1)–M(1)–S(1)	103.92(11)[i]	115.61(12)	113.18(12)	101.41(11)	
N(3)–M(1)–S(1)				118.13(11)	110.22(14)
N(6)–M(1)–S(1)			104.92(12)		
N(2)–M(1)–S(1)	99.19(10)	109.34(12)			
N(1)–M(1)–S(2)	106.15(10)[i]	101.64(11)	114.23(12)	121.53(11)	102.79(14)
N(2)–M(1)–S(2)	112.13(10)	106.18(12)			
N(3)–M(1)–S(2)				106.64(11)	114.70(14)
N(6)–M(1)–S(2)			96.08(12)		
S(2)–M(1)–S(1)	131.32(4)	119.55(6)	126.37(5)	116.87(5)	110.10(9)
Si(1)–S(1)–M(1)	105.30(5)	106.45(7)	95.71(6)	109.42(7)	106.67(10)
Si(2)–S(2)–M(1)	111.42(5)	106.57(7)	110.02(6)	107.92(7)	103.57(10)
Si(3)–S(3)–M(2)			111.70(7)		
Si(4)–S(4)–M(2)			94.63(6)		
S(3)–M(2)–S(4)			124.93(5)		
N(3)–M(2)–S(3)			96.77(12)[iiiii]		
N(4)–M(2)–S(3)			112.32(12)		
N(3)–M(2)–S(4)			104.93(13)[iiiii]		
N(4)–M(2)–S(4)			117.40(12)		
N(4)–M(2)–S(3)			90.32(16)		

Symmetry transformations used to generate equivalent atoms:**1** *i*: x, -y+1/2, -z+1/2; **3** *iiiii:* x+1, y, z

Table S2 Selected interatomic distances (Å) and angles (°) for **6**

Bond length [Å]		Bond angles [deg]	
Ni(1)–N(1)	2.101(5)[a]	N(1)–Ni(1)–N(2)	180[a]
Ni(1)–N(2)	1.988(3)		
Ni(1)–O(1)	2.046(4)[a]	O(1)–Ni(1)–O(1)	180[a]
Ni(1)–O(2)	2.051(4)[a]	O(1)–Ni(1)–O(2)	90.91(16)[a]
Ni(2)–N(4)	2.111(5)		89.09(16)[a]
Ni(2)–N(5)	2.127(5)	O(2)–Ni(1)–O(2)	180[a]
Ni(2)–O(3)	2.059(4)	O(5)–Ni(2)–O(6)	91.41(16)
Ni(2)–O(4)	2.059(4)	O(5)–Ni(2)–O(3)	87.66(16)
Ni(2)–O(5)	2.035(4)	O(6)–Ni(2)–O(3)	178.93(15)
Ni(2)–O(6)	2.047(4)	O(5)–Ni(2)–O(4)	177.97(17)
Ni(3)–N(8)	2.118(5)	O(6)–Ni(2)–O(4)	90.61(16)
Ni(3)–O(7)	2.044(4)[b]	O(3)–Ni(2)–O(4)	90.32(16)
Ni(3)–O(8)	2.044(4)[b]	O(5)–Ni(2)–N(4)	89.67(17)
		O(6)–Ni(2)–N(4)	89.51(18)
		O(3)–Ni(2)–N(4)	89.96(18)
		O(4)–Ni(2)–N(4)	90.51(17)
		O(5)–Ni(2)–N(5)	90.82(18)
		O(6)–Ni(2)–N(5)	87.96(18)
		O(3)–Ni(2)–N(5)	92.58(17)
		O(4)–Ni(2)–N(5)	89.09(18)
		N(4)–Ni(2)–N(5)	177.43(19)
		O(8)–Ni(3)–O(8)	180[b]
		O(8)–Ni(3)–O(7)	88.62(16)[b]
			91.39(16)[b]

				91.38(16) [b]	
				88.61(16) [b]	
	D–H	D–H [Å]	H···A [Å]	D···A [Å]	∠ DHA [°]
1	N1–H1A···O1 [i]	0.86(6)	2.21(6)	2.947(4)	144(5)
	N1–H1B···O6 [i]	0.78(4)	2.18(4)	2.941(5)	165(4)
2	N3–H3D···O1	0.78(5)	2.26(5)	2.961(5)	151(5)
	N3–H3E···O4	0.93(5)	2.16(5)	2.963(5)	143(4)
3	O13–H13A···S2	0.87(9)	2.34(9)	3.179(5)	160(8)
	N6–H6B···O13 [ii]	0.95(6)	2.01(6)	2.955(6)	170(5)
	N3–H3A···O14 [iii]	0.81(7)	2.15(7)	2.954(7)	173(6)
	O14–H14···S3 [iiii]	1.02(10)	2.19(10)	3.188(5)	167(8)
5	O8–H8···O6	0.82	2.06	2.846(6)	159.4
	O9–H9···O8	0.82	1.93	2.680(7)	151.4
	O7–H7···S1	0.83(8)	2.45(9)	3.245(5)	162(8)
			O(7)–Ni(3)–O(7)	180 [b]	
			O(8)–Ni(3)–N(8)	89.59(17)	
			O(8)–Ni(3)–N(8)	90.41(17) [b]	
			O(7)–Ni(3)–N(8)	89.70(17)	
				90.30(17) [b]	
			N(8)–Ni(3)–N(8)	180 [b]	

Symmetry transformations used to generate equivalent atoms: *a*: -x+2, y, -z+2; *b*:- x, y+2, -z+1

Table S3 Hydrogen bonds parameters for complexes **1-3** and **5**.

Symmetry transformations used to generate equivalent atoms:**1** *i*: x, -y+1/2, -z+1/2; **3** *ii*: x, y+1, z; *iii*: x-1,y,z; *iiii*: x, y-1, z

6. References:

1 T. de Neef, *Some applications of series expansions in magnetism* Ph.D. Thesis, Eindhoven, 1975.
2 R. Boča, *Coord. Chem. Rev.*, 2004, **248**, 757−815.
3 R. L. Carlin, *Magnetochemistry*, Springer-Verlag, 1986; O. Kahn, *Molecular Magnetism*, VCH Publishers, Inc., 1993.